ELSEVIER

Biochimica et Biophysica Acta 1460 (2000) 95–105

BIOCHIMICA ET BIOPHYSICA ACTA
BBA

www.elsevier.com/locate/bba

Review paper

NMR probes of vectoriality in the proton-motive photocycle of bacteriorhodopsin: evidence for an 'electrostatic steering' mechanism

Judith Herzfeld *, Brett Tounge

Department of Chemistry, MS #015, Brandeis University, Waltham, MA 02454-9110, USA

Received 21 December 1999; accepted 24 March 2000

Abstract

In recent years, significant progress has been made in elucidating the structure of bacteriorhodopsin. However, the molecular mechanism by which vectorial proton motion is enforced remains unknown. Given the advantages of a protonated Schiff base for both photoisomerization and thermal reisomerization of the chromophore, a five-state proton pump can be rationalized in which the switch in the connectivity of the Schiff base between the two sides of the membrane is decoupled from double bond isomerization. This decoupling requires tight control of the Schiff base until it is deprotonated and decisive release after it is deprotonated. NMR evidence has been obtained for both the tight control and the decisive release: strain develops in the chromophore in the first half of the photocycle and disappears after deprotonation. The strain is associated with a strong interaction between the Schiff base and its counterion, an interaction that is broken when the Schiff base deprotonates. Thus the counterion appears to play a critical role in energy transduction, controlling the Schiff base in the first half of the photocycle by 'electrostatic steering'. NMR also detects other events during the photocycle, but it is argued that these are secondary to the central mechanism.

Keywords: Bacteriorhodopsin; Energy transduction; Proton transport; Nuclear magnetic resonance; Retinal Schiff base; Electrostatic interaction

1. Design for light transduction

The rhodopsins comprise a large class of integral membrane proteins in which a bundle of seven transmembrane helices encapsulates a retinal chromophore that is linked to a buried lysine by a Schiff base (SB). Most of these retinal pigments are signal transducers: the conformational change induced in the protein by photoisomerization of the polyene chain of the chromophore leads to new interactions with cellular species that produce a signaling cascade. A cartoon for such a minimal two-state scheme for signal transduction is shown in Fig. 1.

Unlike most of the rhodopsins, bacteriorhodopsin (bR) is an energy transducer, using light to drive the active transport of protons across the membrane. The scheme shown in Fig. 1 can be expanded to accommodate proton translocation if the two conformations of the pigment differ in both the pK_a of the SB and its connection to proton transport channels on either side of the protein. Two possible variations of such a minimal four-state scheme for energy transduction are shown in Fig. 2. In Fig. 2a it is the protonated SB that is photoisomerized and the unprotonated SB that thermally reisomerizes, while in Fig. 2b it is the unprotonated SB that is photoiso-

* Corresponding author. Fax: +1-617-736-2516;
E-mail: herzfeld@brandeis.edu

0005-2728/00/$ – see front matter
PII: S0005-2728(00)00132-8

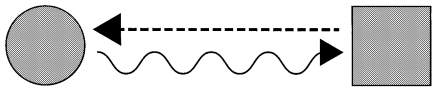

Fig. 1. A minimal two-state scheme for signal transduction by a retinal pigment. The wavy arrow represents photoinduced double bond isomerization in the chromophore and the dotted arrow represents thermal reisomerization of the double bond. The two different shapes represent the two states of the system that conform to the two states of the chromophore. A two-state model has been proposed for signal transduction by rhodopsin, with the circle corresponding to the inactive state and the square corresponding to the active state [37].

merized and the protonated SB that thermally reisomerizes.

The difficulty with the four-state schemes is that the chromophore is unprotonated for one of the two isomerization steps. In fact, a protonated chromophore is important for both photoisomerization and thermal reisomerization. The polyene chain of the protonated chromophore, in contrast to that of the unprotonated chromophore, has resonance structures with relatively closely spaced energy levels (see Fig. 3). This makes thermal isomerization in the protonated chromophore relatively easy [1]. It also shifts photoisomerization in the protonated chromophore to longer wavelengths that are tunable by steric and electric features of the binding site [2]. Due to deprotonation of the chromophore, a pump of the sort in Fig. 2a will not recover effectively and a pump of the sort in Fig. 2b will work only with relatively short wavelength radiation. An example of the latter is the alkaline form of the D85N mutant of bR which pumps protons under blue light [3].

In order to have a protonated chromophore for *both* photoisomerization and thermal isomerization, it is necessary that another type of structural change

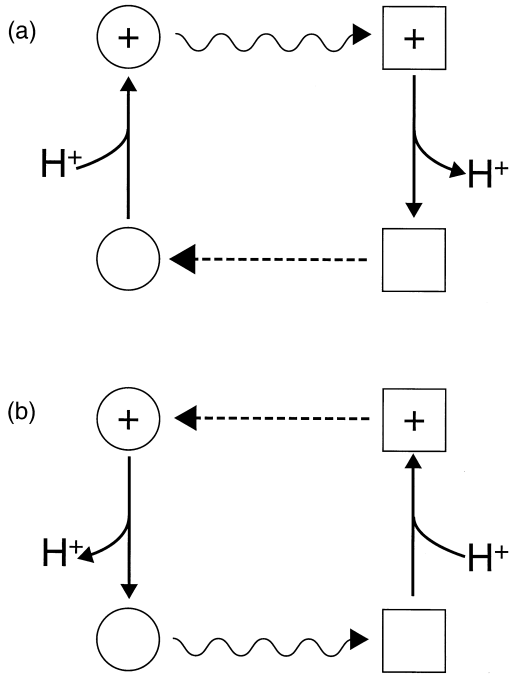

Fig. 2. Two versions of a minimal four-state model for energy transduction by a retinal pigment. The symbols have the same significance as in Fig. 1 except that the presence (absence) of a '+' indicates a protonated (unprotonated) SB, and both the pK_a of the SB and the connectivity of the SB to the two sides of the membrane are switched with isomerization. The scheme in (b) describes proton transport driven by blue light in the D85N mutant of bR (with the circle representing the state in which the SB has a high pK_a and is connected to the intracellular surface, and the square representing the state in which the SB has a low pK_a and is connected to the extracellular surface).

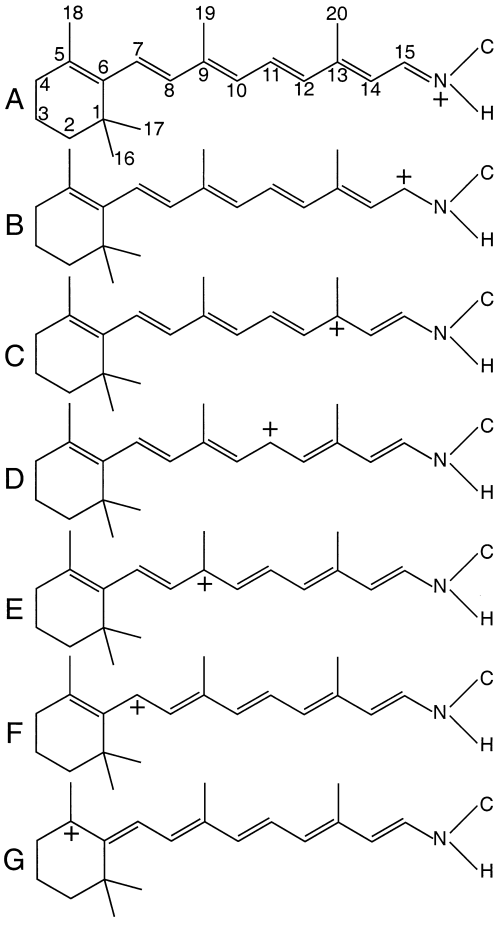

Fig. 3. Resonance structures of protonated Schiff bases of all-trans retinal.

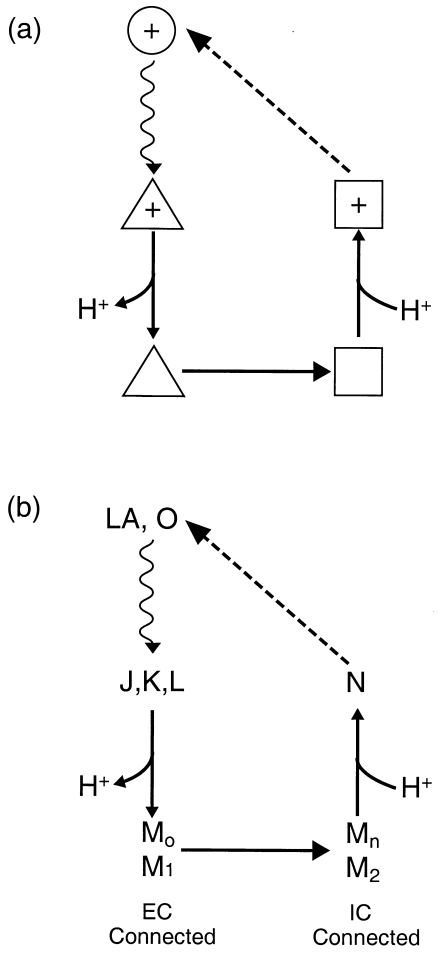

Fig. 4. A minimal five-state model for energy transduction by a retinal pigment with a protonated chromophore in both isomerization steps. The symbols in panel (a) have the same significance as in Fig. 2, except that there is an additional state, represented by a triangle, in which the photoisomerized chromophore, and the protein around it, are prevented from fully relaxing because of the charge on the SB and the CI. In this state, the double bond has isomerized and the pK_a of the SB is reduced, but the connectivity of the SB is not yet switched (so the wavy arrow is vertical and the triangular state is on the left side of the scheme). Panel (b) shows the corresponding intermediates in the proton-motive photocycle of the light adapted (LA) form of wild-type bacteriorhodopsin, beginning with photoisomerization of the retinal from all-trans to 13-cis.

occurs while the SB is deprotonated (so that reprotonation occurs from the other side of the membrane). Such a minimal five-state scheme is shown in Fig. 4. Note that the connectivity of the SB is no longer tightly coupled to the isomeric state of the chromophore; the connectivity switch of the deprotonated SB occurs as an event distinct from double bond isomerization and thus represents a release of strain that the initial photoinduced double bond isomerization produced in the system. Release of strain after SB deprotonation is a reasonable consequence of the loss of the electrostatic interaction of the SB with its counterion (CI). Furthermore, occurring promptly after deprotonation, such a sharp change would be very effective in preventing proton backflow and enforcing the vectoriality of the pump. Consistent with such a mechanism, the largest drop in free energy in the photocycle of wild-type bacteriorhodopsin is found to coincide with the switch in the connectivity of the SB [4]. The drop is large at pH 5 and becomes much larger at pHs above 6.

Electrostatic interactions in the active site of bR are known to be complex. The CI for the protonated SB comprises a hydrogen-bonded complex [5] including the charged residues $D85^-$, $D212^-$ and $R82^+$, as well as water molecules [6,7]. The balance of charge in the active site is critical for order in the region. When both the SB^+ and $D85^-$ are neutralized, as by proton transfer in the $L \rightarrow M$ transition of the photocycle, the chromophore remains well ordered [8]. However, the chromophore becomes disordered when $D85^-$ alone is neutralized, whether by protonation in acid [5] or by mutation [9].

Although proton transfer from the SB^+ to $D85^-$ maintains charge balance, it alters electrostatic interactions. In particular, it releases the electrostatic constraints on the SB and D85. The resulting freedom of the SB is expected to be important for relaxation of strain in the chromophore. In addition, the coupling between helix C (the location of D85) and helix G (the location of the SB site at K216) is expected to be weakened. Although $D212^-$ (a helix turn from K216) and $R82^+$ (a helix turn from D85) remain charged, their highly polar environment provides each with other interaction partners. Reduced coupling between helices C and G may be the factor that allows the helix movements that have been observed in wild-type (WT) bR during the lifetime of the M state [10]. These helix movements have become the marker of the $M_1 \rightarrow M_2$ transition in the WT protein. However, similar helix movement has been effected already in the resting state by the triple mutation D96G (on helix C), F219L (on helix F) and F171C (on helix G) [10]).

With the above considerations in mind, the key to understanding the proton pump mechanism in bR is to understand the difference between the L state, in which the SB is about to release its proton to the extracellular side of the system, and the N state, in which the SB has just accepted a proton from the intracellular side of the system. Alternatively, one can compare the early M state, in which the SB has just released its proton to the extracellular side of the system, to the late M state, in which the SB is about to accept a proton from the intracellular side of the system. In either case, we seek to understand how the SB remains connected to the extracellular side of the system until deprotonation, in spite of the initial photoisomerization of the chromophore.

2. Solid state nuclear magnetic resonance

Nuclear magnetic resonance (NMR) is an attractive method for studying the details of the bR photocycle because chemical shifts and internuclear interactions are sensitive, non-perturbing probes of local structure. Both solution and solid state NMR have been used to examine bR. Solution NMR has the advantage that natural abundance proton signals can be resolved and proton NOEs are beginning to yield distance constraints for bR in its resting state [11]. However, the solution approach has several drawbacks. First, the protein must be dissolved in detergent. Under such conditions, the protein is less stable and its functional status is unclear. By contrast, solid state NMR (SSNMR) can study bR in its native membrane environment. At least as important is the fact that SSNMR can be used to examine photocycle states by trapping them at temperatures far below freezing. This avoids the use of mutants, in which the relationship between the states that accumulate and those in the WT cycle is unclear.

SSNMR includes a growing arsenal of techniques. Cross polarization is used to enhance signal-to-noise and edit spectra. High resolution is obtained by spinning the sample at the magic angle (MAS) which averages the chemical shift and the dipolar interactions to their isotropic values. Recently developed pulse sequences reintroduce dipolar interactions to allow measurement of internuclear distances and dihedral angles [12]. In addition, the development of low temperature MAS probes outfitted with optical fibers has allowed the reproducible in situ accumulation and preservation of different photocycle intermediates [13]. The light adapted, active form of the pigment (LA) is routinely prepared by irradiation with white light at about 0°C. Varying mixtures of the L, early M (M_o), late M (M_n) and N intermediates are then accumulated at lower temperatures by irradiation of LA with long wavelength light [8,14]. The species that are obtained depend on the temperature, the pH, and the salt present (usually 0.1 M NaCl or 0.3 M guanidine·HCl): lower pH favors L over the other states; lower temperatures favor L and M_o over M_n and N; and guanidine·HCl favors M_n over N. Once accumulated, all states are preserved in the dark, at about −100°C, for the duration of data acquisition.

3. View from the Schiff base

The nitrogen SB is at the heart of the action in bR. Fortunately, nitrogen chemical shifts (σ_N) cover a broad range, and this is particularly so of the nitrogen signal of the retinal SB which varies across a range of at least 180 ppm, depending on the protonation state. The resonance is most downfield for a fully deprotonated SB and furthest upfield for a fully protonated SB. Hydrogen bonding produces intermediate chemical shifts that vary according to the sharing of the hydrogen atom: the signal is further downfield when the hydrogen is associated less with the nitrogen, and further upfield when the hydrogen is associated more with the nitrogen. Thus hydrogen bonding of a deprotonated SB (acting as the H acceptor) moves the resonance upfield [15,39,40], while hydrogen bonding of a protonated SB (acting as the H donor) moves the resonance downfield [16,17]. This sensitivity to variations in H bonding makes the SB nitrogen a superb marker for bR photocycle intermediates. In particular, it has so far provided the best way to detect multiple M intermediates [8]. In the deprotonated state, the optical spectrum is relatively insensitive to the chromophore environment and kinetic modeling is necessary to discern more than one M intermediate in time resolved optical spectroscopy of the native protein. In contrast,

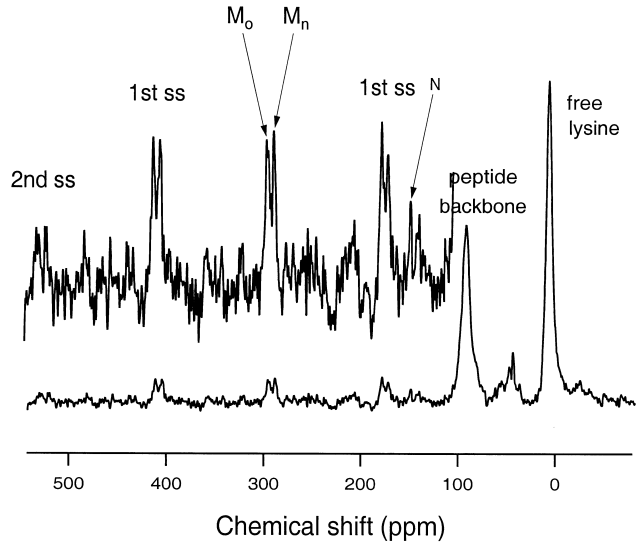

Fig. 5. ^{15}N MAS spectrum of [ζ-^{15}N]lysine labeled bR trapped as a mixture of approximately equal amounts of the M_o and M_n states, with a small amount of the N state. Note that the 8 ppm chemical shift difference for the two M states appears in the centerband and the spinning sidebands (ss). For further details, see Hu et al. [8].

different M intermediates are clearly distinguishable in ^{15}N NMR spectra, as illustrated in Fig. 5.

Table 1 shows the nitrogen chemical shifts for the SB in those bR photocycle intermediates that have been examined so far. These states have been assigned according to the conditions that produce them (pHs, salts, wavelengths) and the observed sequence of thermal relaxation from one state to another. M_o and M_n, the earlier and the later of the two M states that have been observed in NMR studies, may be related to the M_1 and M_2 states identified by other techniques.

What do the nitrogen chemical shifts tell us? Comparing the M_o and M_n states, we see that the hydrogen bonding of the deprotonated SB is stronger (or the pK_a is higher) in the later M than in the earlier M. Thus the SB becomes more disposed to reprotonate in the $M_o \rightarrow M_n$ transition. For the protonated SBs the distance from the nitrogen of the SB to the center of its CI can be estimated from σ_N by calibration against halide salts using the known radii of these anions [14]. This calibration is different for all-trans and 13-cis retinal SBs [17]. The resulting estimates for center-to-center distances are shown in Table 2. We see that the SB^+–CI^- distance decreases markedly from LA to L, indicating a relatively tight electrostatic interaction at the end of the first half of the photocycle. This is consistent with FTIR observations that the SB interacts more strongly with the CI in the L state than in other photocycle intermediates [18–23], including the N intermediate [24]. Table 2 also lists the distances from the SB nitrogen to the nearest carboxylate oxygen from diffraction studies and computer simulations. The computer simulations predict considerable tightening of the SB^+–CI^- interaction over the first half of the photocycle (LA → L), consistent with the NMR results. On the other hand, diffraction

Table 1
^{15}N chemical shifts (σ_N) of the Schiff base in various states of WT bR

Photocycle intermediate	σ_N (ppm)[a]
LA	143.5
L	161
M_o	296.4
M_n	288.8
N	150.7

[a]Referenced to the signal of 5.6 M aqueous $^{15}NH_4Cl$ (which is 26.9 ppm downfield from the signal of liquid ammonia).

Table 2
Estimates of the SB^+–CI^- distances (in Å) for various photocycle intermediates

	LA state	K state	L state	N state
NMR	4.08		3.50	3.68
Simulations[a]				
Scharnagl et al.	4.35		3.44	3.32
Schulten et al.	3.71		3.23	
Diffraction[b]				
2BRD (3.5 Å)	3.71			
1BRR (2.9 Å)	3.50			
	3.59			
	3.35			
1BRX (2.3 Å)	3.66			
1CWQ (2.25 Å)	3.74			
1C3W (1.55 Å)	3.74			
1QHJ (1.9 Å)	3.65			
1QKO (2.1 Å)		3.89		
1QKP (2.1 Å)	3.56	3.85		

The NMR distances are based on σ_N values calibrated against model compounds [17] and the other distances are from the SB nitrogen to the nearest carboxylate oxygen.
[a]Coordinates kindly supplied by principal investigators.
[b]Structures are from the Protein Data Bank.

results suggest that some loosening may occur first ($LA \rightarrow K$).

The interaction of the SB with its CI is one of four mechanisms that have been proposed for 'tuning' retinal pigments [2,25]. The weaker the SB–CI interaction, the more readily the charge on the chromophore can delocalize (see Fig. 3), the lower the energy of the excited state, and the longer the wavelength of maximum visible absorption (λ_{max}). The three other potential tuning mechanisms are steric effects on the planarity of the π-system, electrostatic effects of nearby charges or partial charges, and the polarizability of the local environment. When these three mechanisms are constant, λ_{max} is controlled entirely by the SB–CI interaction and a common linear relationship between $\nu_{max} = c/\lambda_{max}$ and the σ_N of the SB has been found for fully planar retinal SB compounds and all the forms of bR that have been examined so far except the L intermediate [13]. Whereas the N intermediate has roughly the expected λ_{max} (560 nm) for fully planar 13-cis retinal SB with the observed σ_N, the L intermediate has a similar λ_{max} (550 nm) in spite of a significantly stronger SB–CI interaction (one that corresponds to $\lambda_{max} \sim 491$ nm in model compounds). This indicates that there is strain in the chromophore in the L state, which has dissipated before the N state. Distortion in the L chromophore has also been inferred from FTIR [19,24,26,27] and resonance Raman [28] spectra, and is predicted by molecular dynamics simulations [29–31].

Where might the strain in the L chromophore be located? For a retinal SB with a strong SB–CI interaction, charge delocalization is difficult and the dominant resonance structure is expected to be the one with the positive charge on C_{15} and a single bond to the nitrogen. The energy of this state will be closer to that of the ground state (and λ_{max} will be larger) if strain around the C_{15}–N bond favors the lower bond order. Thus, the anomalous relationship between λ_{max} and σ_N in the L intermediate suggests strain around the C_{15}–N bond that is relaxed in the N state.

The progress of the relaxation of the chromophore through the three steps $L \rightarrow M_o \rightarrow M_n \rightarrow N$ is unknown. However, there is evidence that relaxation is complete in the first two steps, consistent with the release of electrostatic constraints once the SB proton has been transferred to D85. A model for a fully relaxed M state can be found in the alkaline form of the D85N mutant where D85 has been neutralized by mutation and the SB has been neutralized by titration. The σ_N of the SB in this fully relaxed system is essentially identical to that in the M_n state of the WT, 8 ppm upfield from that of the M_o state. Thus, it appears that chromophore relaxation occurs in the same period as the switch in the SB connectivity and is therefore likely to be mechanistically significant.

4. View around the retinal binding pocket

Due to its inverse cubed dependence on distance, the dipolar interaction provides a more precise measure of internuclear distances than is currently feasible by diffraction. However, MAS averages the dipolar interaction to zero (its isotropic value) and we need MAS to average the shift anisotropy for high resolution. Fortunately, it turns out that 'we can have our cake and eat it too': specific pulse sequences that are synchronous with MAS can manipulate the spins in such a way as to defeat the averaging of the dipolar interactions, without defeating the averaging of the chemical shift anisotropy [12].

The first use of such recoupling methods for measuring internuclear distances from the chromophore to nearby amino acids in bR has been for ^{13}C labels at the 14-carbon of the retinal and the 4-carbon of the aspartic acid residues [32]. Using RF-driven recoupling, it was found that the distance between the 14-^{13}C in the retinal and the 4-^{13}C in D212 is 4.4 ± 0.6 Å in LA and 4.8 ± 1.0 Å in M_o. For all the other aspartic acid residues, including D85, the distance to the retinal is > 6.0 Å in both states. The increase in the D212–retinal distance is small and within the experimental error. However, spin diffusion experiments independently indicate a $16 \pm 10\%$ increase in distance [32].

In Tables 3 and 4, the NMR distances are compared with those obtained in simulations and diffraction experiments. Close agreement is found for the LA state of WT bR and similar distances have been found for the resting state of the D96N mutant. A much longer distance to D212 has been found by diffraction for the M_N state of D96N than found by NMR for the M_o state of the WT pigment. The

M_N state of D96N is thought to be an N-like state in which the SB has remained deprotonated due to the absence of the normal proton donor. The closest analog in the WT photocycle would be the M_n state. If the correspondence is good, then a large change in the D212–retinal distance is expected in the $M_o \rightarrow M_n$ transition, from the 4.8 Å measured for M_o of the WT in the NMR experiments to the 5.8 Å found for M_N of D96N in the diffraction experiments. This suggests that relaxation of the chromophore in the $M_o \rightarrow M_n$ transition is accompanied by a much larger movement of the neutralized SB end of the chromophore away from its neutralized CI than occurs earlier, in the $L \rightarrow M_o$ transition, consistent with an electrostatic release mechanism. An NMR measurement of the actual M_n distance is underway.

The binding pocket is also well populated with tryptophan residues: among the eight tryptophan residues in the protein, W182 and W86 sandwich the polyene chain on the cytoplasmic and extracellular sides, respectively, and W189 neighbors the ionone ring. Of these tryptophans, the indole ring of W182 is close enough to the 19- and 20-methyl groups of the retinal for NMR distance measurements. The first tryptophan distance measurement has used ^{13}C in the 20-methyl group of the retinal and ^{15}N in the indole rings of the tryptophan sidechains. In the LA and MO states, recoupling of the heteronuclear dipolar interaction using the REDOR pulse sequence produced dephasing of the ^{13}C at a rate corresponding to distances from the ^{15}N of W182 of 3.36 ± 0.2 Å and 3.16 ± 0.4 Å respectively [38]. These values are in the range of the diffraction distances (see Table 5).

Table 3
Distances from [14-C]retinal to [4-C]D212 (in Å) for various photocycle intermediates of bR

	LA state	L or M_o or M_1 state	M_n or M_N or M_2 state
NMR, WT[a]	4.4 ± 0.6	4.8 ± 1.0	
Simulations, WT[b]			
Scharnagl et al.	4.19	$4.23 \rightarrow 5.47 \rightarrow 5.48$	$4.94 \rightarrow 4.93$
Schulten et al.	5.65	5.68	
Diffraction, WT[c]			
2BRD (3.5 Å)	4.29		
1BRR (2.9 Å)	4.45		
	4.50		
	4.33		
1BRX (2.3 Å)	4.40		
1CWQ (2.25 Å)	4.45		
1C3W (1.55 Å)	4.33		
1QHJ (1.9 Å)	4.41		
1QKP (2.1 Å)	4.66		
Diffraction, D96N[c]			
1C8R (1.8 Å)	4.52		
1C8S (2.0 Å)			5.79

[a]Derived from RF-driven recoupling experiments [32].
[b]Coordinates kindly supplied by principal investigators.
[c]Structures are from the Protein Data Bank.

Table 4
Distances from [14-C]retinal to [4-C]D85 (in Å) for various photocycle intermediates of bR

	LA state	L or M_o or M_1 state	M_n or M_N or M_2 state
NMR, WT[a]	>6	>6	
Simulations, WT[b]			
Scharnagl et al.	6.22	$7.65 \rightarrow 8.25 \rightarrow 7.77$	$7.68 \rightarrow 7.88$
Schulten et al.	5.61	5.57	
Diffraction, WT[c]			
2BRD (3.5 Å)	5.13		
1BRR (2.9 Å)	6.28		
	6.25		
	6.43		
1BRX (2.3 Å)	5.75		
1CWQ (2.25 Å)	5.62		
1C3W (1.55 Å)	5.69		
1QHJ (1.9 Å)	4.28		
1QKP (2.1 Å)	5.63		
Diffraction, D96N[c]			
1C8R (1.8 Å)	5.87		
1C8S (2.0 Å)			7.17

[a]Derived from RF-driven recoupling experiments [32].
[b]Coordinates kindly supplied by principal investigators.
[c]Structures are from the Protein Data Bank.

5. View in the peptide backbone

As discussed above, diffraction studies have found some rearrangement of the helices of WT bR in the late M state. Corresponding changes on the local level can be examined by NMR using ^{13}C and ^{15}N labels in the peptide backbone. As it happens, among the 248 residues in bR, the 21 valine residues are particularly concentrated in the F and G helices, which are the helices that show the most change in diffraction studies. Changes in peptide bonds of the valine residues have been examined by ^{13}C NMR

Table 5
Distance from [20-C]retinal to [indole-N]W182 (in Å) in wild-type bR

	LA state	Photocycle intermediates
NMR[a]	3.36 ± 0.2	3.16 ± 0.4 (M_o)
Simulations[b]		
Scharnagl et al.	4.02	3.57 (L) → 3.42 → 3.43 → 3.42 → 3.48 → 3.18 (N)
Schulten et al.	3.66	3.73 or 3.47 (L)
Diffraction[c]		
2BRD (3.5 Å)	3.66	
1BRR (2.9 Å)	3.75	
	3.45	
	3.58	
1BRX (2.3 Å)	3.84	
1CWQ (2.25 Å)	3.47	3.41 (M)
1C3W (1.55 Å)	3.35	
1QHJ (1.9 Å)	3.27	
1QKO (2.1 Å)		2.79 (K)
1QKP (2.1 Å)	3.36	
Diffraction, D96N[c]		
1C8R (1.8 Å)	3.17	
1C8S (2.0 Å)		3.55 (M)

[a]Derived from REDOR recoupling experiments [38].
[b]Coordinates kindly supplied by principal investigators.
[c]Structures are from the Protein Data Bank.

difference spectroscopy of [1-^{13}C]valine labeled bR [8]. Out of the 21 valine residues, it was found that two resonances are shifted upfield in the LA–M_o difference spectrum, corresponding to looser H bonding, and a different two resonances are shifted downfield in the LA–M_n difference spectrum corresponding to tighter H bonding. This indicates that while most of the 21 valine residues remain unperturbed relative to the LA state, at least two are perturbed in the M_o state, and all of these perturbations relax in the $M_o \rightarrow M_n$ transition while at least two other valine residues become perturbed. Thus, the difference spectra show energy moving around the peptide backbone during the $M_o \rightarrow M_n$ transition, consistent with the possibility of a protein conformational change. All four of the changes in the $M_o \rightarrow M_n$ transition correspond to tightening H-bonds: two represent recovery from earlier loosening of H-bonds that were relatively tight in the LA state, and two represent tightening of H-bonds that were relatively loose in the LA state.

Whereas the hydrophobic valine residues tend to be buried in the protein, the hydrophilic arginine residues tend to be located at the surface. Changes in arginine peptide bonds have been examined in [U-^{15}N]arginine labeled bR and the LA–M_o difference spectrum shows that two resonances are shifted downfield (Petkova, unpublished results). Thus changes in the hydrogen bonding of the amide nitrogen occur in at least two of the seven arginine residues in the LA → M_o transition. It remains to be seen whether these recover in the $M_o \rightarrow M_n$ transition and whether new perturbations appear.

6. View in the extracellular transport channel

The extracellular half of the proton transport channel is the most open part of the bR structure. This is presumably why the SB proton freely exchanges with bulk water protons within 0.5 ms [7]. The half-channel includes the elements of the SB counterion at one end, and a cluster of surface residues that act as the 'proton release group' at the other end. R82 is located about midway along the half-channel and, with its long sidechain, it can either participate in the SB counterion or interact with the proton release group. Indeed, molecular dynamics simulations predicted that when D85 is protonated, the sidechain of R82 swings away from the SB and toward the extracellular surface [30,31,33]. This would have the effect of decreasing the pK_a of the proton release group and promoting proton discharge.

^{15}N SSNMR has been used to examine the behavior of the sidechains of the seven arginine residues in bR [34]. The most notable observation was that, while in LA all seven arginine residues have the small to moderate degrees of guanidyl asymmetry typically observed in proteins, in the M_o and M_n states one of the residues becomes extraordinarily asymmetric (as shown in Fig. 6). This is consistent with a change from an ordinary hydrogen-bonding environment to one in which the hydrogen bonding is extremely lopsided. Interestingly, the NMR signal of a highly asymmetric arginine is also observed in the D85N mutant, both at alkaline pHs where the SB is deprotonated and at neutral pHs where the SB is protonated. Since D85 is just one helix turn from R82, the asymmetric NMR signal was assigned to R82. This is consistent with the molecular dynamics prediction of

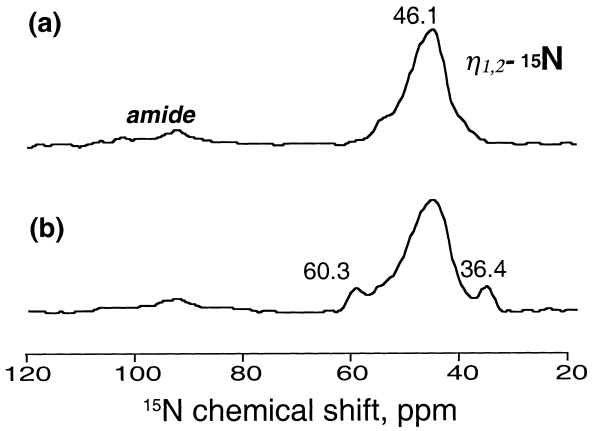

Fig. 6. ^{15}N MAS spectrum of [$\eta_{1,2}$-^{15}N]arginine labeled bR trapped in (a) the LA state and (b) the M_o state. Using spin diffusion, it has been determined that the 'wing peaks' in the M_o spectrum are from ^{15}N nuclei on the same arginine residue. For further details, see Petkova et al. [34].

movement of R82 once D85 is neutralized. Repositioning of the R82 sidechain has also been detected in recent diffraction studies of the D96N mutant [35]. Furthermore, this rearrangement was found to result in a drastic change in the hydrogen bonding of R82. In the resting state of D96N, the guanidyl nitrogens of R82 are found to be thoroughly hydrogen bonded. But in the M_N state of D96N, one of the terminal nitrogens of R82 seems to lack any hydrogen-bonding partner. This is consistent with the extreme asymmetry observed in the NMR signal whenever D85 is protonated and confirms the NMR assignment to R82.

7. The proton pump mechanism – electrostatic steering

SSNMR studies of bR have detected changes in the chromophore, in the extracellular half of the transport channel, and in the peptide backbone. Of these, the changes in the chromophore are probably the most important for energy transduction.

The asymmetric arginine signal that has been assigned to R82 in the extracellular half-channel is already present in the M_o state and cannot be part of the connectivity switch unless the change in connectivity occurs in the $L \rightarrow M_o$ transition, rather than in the $M_o \rightarrow M_n$ transition. Even then, it seems unlikely that the change in R82 could be the thermodynamically irreversible step responsible for enforcing vectorial transport. The distinctively asymmetric arginine signal is found in the D85N mutant, whether the SB is protonated or not. Nevertheless, the alkaline form of D85N pumps protons in the normal direction when irradiated with blue light (see the above discussion of Fig. 2).

The NMR changes detected in the peptide backbone probably reflect the helix movements that have been seen in diffraction experiments. The significance of these helix movements for proton transport is currently being reassessed. Two roles have been discussed. One is that hydrogen-bonding changes associated with the helix movements are responsible for the switch in connectivity of the SB from the half-channel on one side of the membrane to the half-channel on the other side. Another possibility is that the helix movements facilitate reprotonation of the SB. In the resting state, the proton donor, D96, is isolated in a hydrophobic pocket and no proton transport pathway is evident to connect it to the SB. Helix movement on the cytoplasmic side opens the region between the helices somewhat and may accommodate enough water molecules to form a transient H-bonded chain between D96 and the SB.

Only the second of the two proposals for the significance of helix movements survives the most recent structural studies. Since the open conformation has been observed after SB deprotonation in every active bR variant that has been examined, it may be important for facilitating SB reprotonation. However, in some active mutants, the open conformation is also present, or even dominant, prior to SB deprotonation [10,36]. In these systems helix movement cannot be responsible for the connectivity switch, and a more subtle change in the active site seems more likely to be responsible. Since such local change suffices to enforce vectoriality for some mutants, there is no reason to invoke a different mechanism for the WT. Thus, although the backbone changes are useful as markers of the early and late M states in WT bR, they are probably not significant for the switch in SB connectivity.

The changes in the chromophore itself are consistent with a subtle, local mechanism for control of SB connectivity. First of all, the L chromophore shows strain that is gone in the N chromophore. The M_n

state also appears to be fully relaxed, indicating that the strain in the chromophore is relieved before SB reprotonation. Some of the relaxation clearly occurs in the $M_o \rightarrow M_n$ transition because the nitrogen signal shows a change in SB hydrogen bonding during this step. Whether some of the relaxation also occurs in the $L \rightarrow M_o$ transition depends on how early an M state the M_o state is. If the L and M_o chromophores differ only in the protonation state of the SB, then all the chromophore relaxation occurs in the $M_o \rightarrow M_n$ transition and coincides with the switch in the connectivity of the SB. Future measurements comparing the L and M_o chromophores should settle this question.

Two pieces of evidence suggest that the strain in the L chromophore is due to electrostatic interaction with the CI, rather than steric effects in the binding pocket. First, the NMR data indicate that the SB^+–CI^- interaction is relatively strong in the L state. Second, the strain in the chromophore is released when the electrostatic interaction is broken by proton transfer from the SB^+ to the CI^-. This is also when the connectivity of the SB switches from the extracellular half-channel to the intracellular half-channel. Therefore, it seems likely that interaction with the CI is responsible for keeping the SB connected to the extracellular side of the membrane during the first half of the photocycle, in spite of photoisomerization of the chromophore. Moreover, the strain that this 'electrostatic steering' produces in the chromophore is expected to cause a sharp rearrangement when the electrostatic yoke is broken. Such a strongly irreversible step would make the pump effective over a very wide pH range. Thus 'electrostatic steering' can connect the timing of the switch in SB connectivity with the irreversibility that is at the heart of vectorial action in light-driven proton transport by bR.

References

[1] E. Tajkhorshid, B. Paizs, S. Suhai, J. Phys. Chem. B 103 (1999) 4518–4527.

[2] J. Hu, R.G. Griffin, J. Herzfeld, Proc. Natl. Acad. Sci. USA 91 (1994) 8880–8884.

[3] J. Tittor, D. Oesterhelt, E. Bamberg, Biophys. Chem. 56 (1995) 153–157.

[4] K. Ludmann, C. Gergely, G. Varo, Biophys. J. 75 (1998) 3110–3119.

[5] H.J.M. de Groot, S.O. Smith, J. Courtin, E. Van den Berg, C. Winkel, J. Lugtenburg, R.G. Griffin, J. Herzfeld, Biochemistry 29 (1990) 6873–6883.

[6] S. Subramaniam, Curr. Opin. Struct. Biol. 9 (1999) 462–468.

[7] G.S. Harbison, J.E. Roberts, J. Herzfeld, R.G. Griffin, J. Am. Chem. Soc. 110 (1988) 7221–7223.

[8] J.G. Hu, B.Q. Sun, M. Bizounok, M.E. Hatcher, J.C. Lansing, J. Raap, P.J.E. Verdegem, J. Lugtenburg, R.G. Griffin, J. Herzfeld, Biochemistry 37 (1998) 8088–8096.

[9] M.E. Hatcher, J.G. Hu, M. Belenky, P. Verdegem, J. Lugtenburg, R.G. Griffin, J. Herzfeld (2000), to be submitted.

[10] S. Subramaniam, I. Lindahl, P. Bullough, A.R. Faruqi, J. Tittor, D. Oesterhelt, L. Brown, J. Lanyi, R. Henderson, J. Mol. Biol. 287 (1999) 145–161.

[11] H. Patzelt, A.S. Ulrich, H. Egbringhoff, P. Dux, J. Ashurst, B. Simon, H. Oschkinat, D. Oesterhelt, J. Biomol. NMR 10 (1997) 95–106.

[12] R.G. Griffin, Nat. Struct. Biol. 5 (1998) 508–512.

[13] J.G. Hu, B.Q. Sun, R.G. Griffin, J. Herzfeld, Biophys. J. 70 (1996) A107.

[14] J.G. Hu, B.Q. Sun, A.T. Petkova, R.G. Griffin, J. Herzfeld, Biochemistry 36 (1997) 9316–9322.

[15] P.W. Westerman, R.E. Botto, J.D. Roberts, J. Org. Chem. 43 (1978) 2590–2596.

[16] H.J.M. de Groot, G.S. Harbison, J. Herzfeld, R.G. Griffin, Biochemistry 28 (1989) 3346–3353.

[17] J.G. Hu, R.G. Griffin, J. Herzfeld, J. Am. Chem. Soc. 119 (1997) 9495–9498.

[18] H. Kandori, Y. Yamazaki, J. Sasaki, R. Needleman, J.K. Lanyi, A. Maeda, J. Am. Chem. Soc. 117 (1995) 2118–2119.

[19] A. Maeda, J. Sasaki, J.M. Pfefferle, Y. Shichida, T. Yoshizawa, Photochem. Photobiol. 54 (1991) 911–921.

[20] A. Maeda, J. Sasaki, Y. Shichida, T. Yoshizawa, Biochemistry 31 (1992) 462–467.

[21] A. Maeda, J. Sasaki, Y. Yamazaki, R. Needleman, J.K. Lanyi, Biochemistry 33 (1994) 1713–1717.

[22] Y. Yamazaki, M. Hatanaka, H. Kandori, J. Sasaki, W.F.J. Karstens, J. Raap, J. Lugtenburg, M. Bizounok, J. Herzfeld, R. Needleman, J. Lanyi, A. Meada, Biochemistry 34 (1995) 7088–7093.

[23] Y. Yamazaki, S. Tuzi, H. Saito, H. Kandori, R. Needleman, J.K. Lanyi, A. Maeda, Biochemistry 35 (1996) 4063–4068.

[24] J.M. Pfefferle, A. Maeda, J. Sasaki, T. Yoshizawa, Biochemistry 30 (1991) 6548–6556.

[25] A. Kropf, R. Hubbard, Ann. N.Y. Acad. Sci. 74 (1958) 266–280.

[26] K. Fahmy, F. Siebert, M.F. Grossjean, P. Tavan, J. Mol. Struct. 214 (1989) 257–288.

[27] O. Weidlich, F. Siebert, Appl. Spectrosc. 47 (1993) 1394–1400.

[28] R. Lohrmann, M. Stockburger, J. Raman Spectrosc. 23 (1992) 575–583.

[29] W. Humphrey, D. Xu, M. Sheves, K. Schulten, J. Phys. Chem. 99 (1995) 14549–14560.

[30] C. Scharnagl, J. Hettenkofer, S.F. Fischer, Int. J. Quantum Chem. Quantum Biol. Symp. 21 (1994) 33–56.
[31] C. Scharnagl, J. Hettenkofer, S.F. Fischer, J. Phys. Chem. 99 (1995) 7787–7800.
[32] J.M. Griffiths, A.E. Bennett, M. Engelhard, F. Siebert, J. Raap, L. Lugtenburg, J. Herzfeld, R.G. Griffin, Biochemistry 39 (1999) 362–371.
[33] C. Scharnagl, S.F. Fischer, Chem. Phys. 212 (1996) 231–246.
[34] A.T. Petkova, J.G. Hu, M. Bizounok, M. Simpson, R.G. Griffin, J. Herzfeld, Biochemistry 38 (1999) 1562–1572.
[35] H. Luecke, B. Schobert, H.-T. Richter, J.-P. Cartailler, J.K. Lanyi, Science 286 (1999) 255–260.
[36] J. Tittor, S. Paula, S. Subramaniam, J. Heberle, R. Henderson, D. Oesterhelt, Biophys. J. 78 (2000) 478A.
[37] V.R. Rao, D.D. Oprian, Annu. Rev. Biophys. Biomol. Struct. 25 (1996) 287–314.
[38] A.T. Petkova, C.P. Jaroniec, M. Hatanaka, J.G. Hu, M. Belenky, M. Verhoeven, J. Lugtenburg, R.G. Griffin, J Herzfeld (2000) to be submitted.
[39] D.D. Muccio, W.G. Copan, W.W. Abrahamson, G.D. Mateescu, Org. Magn. Res. 22 (1984) 121–124.
[40] J. Sitkowski, L. Stetaniak, I. Wawer, L. Kaczmarek, G.A. Webb, Solid State NMR 7 (1996) 83–84.